sciendo

Strojnícky časopis – *Journal of* MECHANICAL ENGINEERING,
VOL 73 (2023), NO 1, 25 - 42

STU SjF

A BEE COLONY NEURO-FUZZY CONTROLLER TO IMPROVE WELL PREMIXED COMBUSTION

DEBBAH Abdesselam[1*], KELAIAIA Ridha[2], KERBOUA Adlen[3]

[1]L2RCS Laboratory, University of Badji Mokhtar-Annaba, Algeria ,
Department of Petrochemical engineering, University of 20 August 1955-Skikda, PB N° 26 Route Elhadaik, Skikda ,21000, Algeria, e-mail: a.debbah@univ-skikda.dz
[2]GMM Laboratory, Department of mechanical engineering, University of 20 August 1955-Skikda , PB N° 26 Route Elhadaik, Skikda, 21000, Algeria e-mail: r.kelaiaia@univ-skikda.dz
[3]Department of Petrochemical engineering, University of 20 August 1955-Skikda, PB N° 26 Route Elhadaik, Skikda, 21000, Algeria. e-mail: ad.kerboua@univ-skikda.dz

Abstract: In order to actively control combustion reaction, this study proposes an adaptive neuro-fuzzy (ANFIS) control scheme of interaction between premixed combustion reaction and acoustic flame perturbation where the flame pressure movement will be considered as model perturbation. Using the Cantera database, it is possible to investigate the mechanisms by which the combustion process interacts with acoustic, vorticity, and entropy waves. A well-stirred reactor (WSR) has been extensively used to model combustion processes in three different reaction zone regimes. We designed the control architecture to achieve an intelligent representation of the system for various operating scenarios, which was motivated by the complexity of the mathematical model that was being used. This goal is accomplished by an artificial bee colony (ABC), which uses simulated data from a mathematical model to optimize a neuro-fuzzy with less computational expense. The optimized neuro-fuzzy identifier is converted to an adaptive neural-based (ANFIS) controller optimized to control the outputs of the system. In keeping with the combustion temperature set point, the results demonstrate a remarkable attenuation of flame perturbation and acceptable combustion reaction quality (NOx emission).

KEYWORDS: Combustion, Flame perturbation, Well stirred reactor, Neuro-fuzzy adaptive control, Artificial bee colony Optimization.

1 Introduction

As a result of growing awareness of the effects of greenhouse gases on climate change, government organizations have recently been pressed to limit the amounts of carbon monoxide and carbon dioxide released into the atmosphere by engines [1]. Nitric oxide (NO) and nitrogen dioxide (NO2), both of which are created during combustion emissions, are the nitrogen oxides that are referred to as the problem with industrial growing. Lean local combustion results in a reduction in NOx emissions [2] and can be used to lower flame temperature. Lean premixed fuels are prone to combustion perturbation even though it is anticipated that they will play a significant role in the reduction of emissions. According to a number of earlier studies, it is possible to model flame-acoustic interactions in this regime by expanding the steady-state well stirred reactor (WSR) equations to take non-steady effects into account. By assuming that all spatial quantities are uniform, it is possible to derive these unsteady reactor equations from a simple spatial integration of the conservation equations over the WSR region. When the acoustic field and pressure oscillations are in phase, the unsteady heat release from the disturbances increases the field's energy [3]. These oscillations have a variety of negative effects, including increased vibration, shortened part lives, blow-off

DOI: 10.2478/scjme-2023-0003, Print ISSN 0039-2472, On-line ISSN 2450-5471

or flashback, and occasionally even total system failure. There is a vast amount of literature on the related unsteady combustion issues of combustion noise, inherent flame instabilities, acoustic-flame interactions, and combustion system instabilities. As a result, there is no attempt in this paper to address each of these problems. Instead, its focus is on the interactions between premixed flames and acoustic waves without taking into account the broader system in which they occur. In addition to the books and review articles that appear in this issue, take note of the numerous additional publications that address related issues in unsteady combustion and combustion instability. The traditional and most often used controllers in the engine sector are the proportional integral derivative (PID) and its modified schemes [4],[5]. Linear quadratic gaussian (LQG) [6],[7] is an optimal control method. The precise linear state-space models required for a real engine combustor are absent, though. Since new generations of state-space identification techniques will be marketed in the future, this scenario will change. It is also possible to use more sophisticated techniques to regulate an unstable combustor, such as fuzzy logic [8], neural networks [9], [10], robust (H, H2) [11], [12], adaptive [13], and predictive (hybrid) [14], [15]. Generally, there is a wealth of literature on robust sliding mode control [16 – 18]. Identifying a well stirred reactor (WSR) subject to limit cycle oscillations for three distributed possible cases is the first contribution of this paper. The second contribution involves creating an intelligent adaptive control to actuate a fuel valve to stabilize an unstable lean premixed combustion, which poses a challenging problem for control system design primarily due to the significant dead time phase delay and noise in the combustion process. Other characteristics of combustor, besides a significant phase delay and noise, include amplitude modulations and net random phase walks, which may be crucial in the control strategy. An improved adaptive neural controller that performs well in a variety of operating conditions and has a great deal of potential to change dynamics for a practical application is made using the suggested modeling architecture. The suggested improved controller has generated some interest because it can achieve rapid response, strong transient performance, and robustness with regard to changes in the combustor's characteristics and modelled disturbances [1],[19]. The paper is organized as follows: the first section is an overview of recent research as well as combustor and unsteady flame control. The mathematical model was presented in the second section. Thermo-acoustic stability was the main focus of Section 3; Section 4 is devoted to the optimization of the neuro-fuzzy controller; and Section 5 discusses the simulation and the outcomes. The conclusion was finally the focus of the last paragraph.

2 Combustor Model

The lumped and accurate architecture was adopted to test and validate the mathematical model of the proposed combustion system. The Well Stirred Reactor (WSR) reaction model, which emphasizes the flame's transient responses, has been employed in the majority of earlier combustion models. The Well Stirred Reactor (WSR) reaction model, which centers on the transition dynamics of the flame, has been used in several previous combustion models. This reaction model (WSR) cannot explain several combustion behavior in the combustor, but it can acknowledge that mixing time is less than the chemical reaction time. Consequently, inside the combustor volume, the physical proprieties are assumed to be uniform and the characteristics of the flame and the magnitude of instability heat release can be identified. Another advantage of this approach is its ability to subjoin the thermo-acoustic model to the combustor model.

Table 1. Specifications of the combustor model.

Parameters	Value	Unit
Equivalence ratio	0.45 - 1	NA
Combustor pressure	1	bar
Inlet length	428	mm
Combustor diameter	184	mm
Combustor length	854	mm

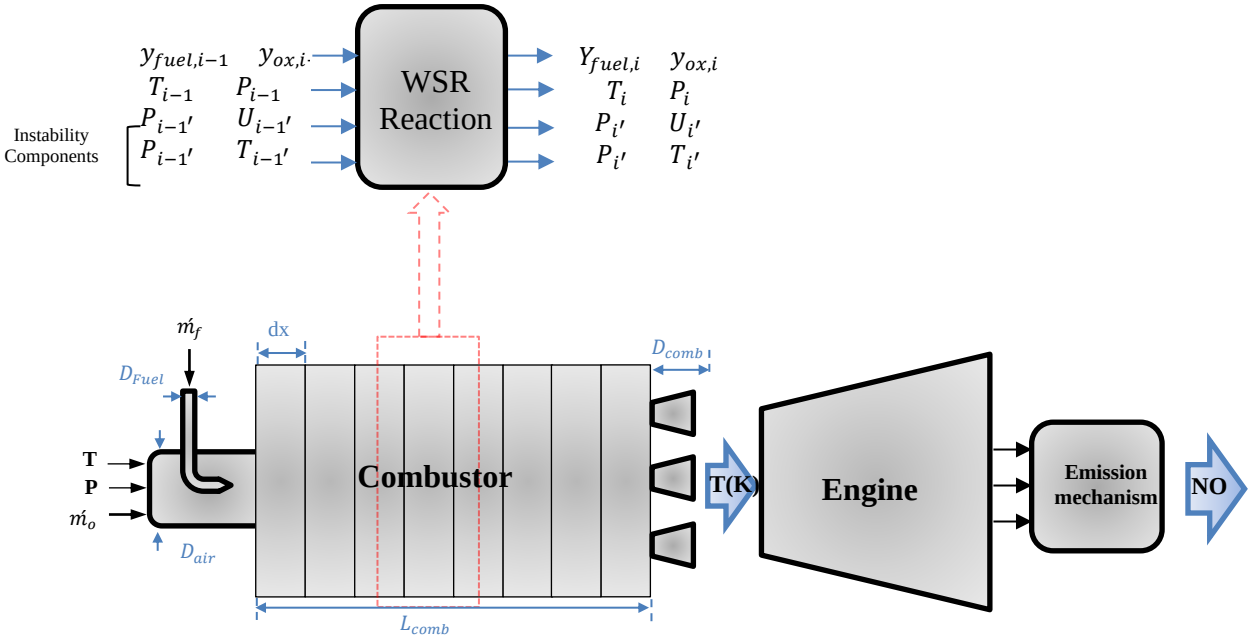


Fig .1 Schematic of the proposed combustor.

Fig.1 shows the combustor overall schematic used in this paper. The combustion temperature characteristics can be estimated when the mass fraction of oxidizer (Air) and fuel (CH_4) are diffused.

2.1 Well stirred reactor (WSR)

The variation of the mass fraction rate of oxidizer (Air) and fuel (CH_4) regarding time is modeled by using the chemical species and mass conservation equations, which lead to two governing equations of two state variables (1) and (2). Then, the result of a chemical reaction is characterized in a balance case using the specifications of the mass fraction. Based on the equation of species conservation, we found the dynamical equation of fuel, oxidizer, and products in equation (4) [20].

$$\boldsymbol{Fuel}: \quad \rho V \frac{dy_{fuel}}{dt} = \left(y_{fuel,in} - y_{fuel}\right)\dot{m}_{in} + MW_{fuel}\dot{\omega}_{fuel}V \tag{1}$$

$$\boldsymbol{Oxidizer}: \quad \rho V \frac{dy_{oxid}}{dt} = \left(y_{oxid,in} - y_{oxid}\right)\dot{m}_{in} + MW_{fuel}\frac{y_{oxid,in}}{y_{fuel,in}}\dot{\omega}_{fuel}V \tag{2}$$

$$\boldsymbol{Energy}: \quad \frac{dT}{dt} = -\frac{1}{c_{p,mix}}\left[\sum_j \frac{dy_j}{dt}\left(h_j - \frac{R_u T}{MW_J}\right) + \frac{\dot{m}_{in}}{\rho V}(h - h_{in}) - \frac{1}{\rho}\frac{dp}{dt}\right] \tag{3}$$

$$\textbf{\textit{Product}}: \quad y_{prod} = 1 - y_{fuel} - y_{oxid} \tag{4}$$

The temperature, the desired output state from the combustor model, determines all of these states. In order to solve equation (3), temperature is substituted for internal energy and enthalpy. The limitation of the enthalpy difference between the input and output of the combustor volume, however, makes the model critical. It is because of the complicated estimation of temperature variation effects on the equivalence ratio inside the combustion chamber. For this reason, we need to satisfy the quasi-steady state, composition data on the equivalence ratio in the output of the combustion chamber. The oscillations of flow rate produce the equivalence ratio ϕ oscillations illustrated in the following linearized equation that is considered as the equivalence ratio ϕ definition:

$$\frac{\acute{\phi}}{\bar{\phi}} = \frac{\acute{m}_f}{\bar{m}_f} - \frac{\acute{m}_o}{\bar{m}_o} \tag{5}$$

With $\dot{\bar{m}}_i$ representing the flow mass of air and fuel in the case of stationary fluid (i=o,f).

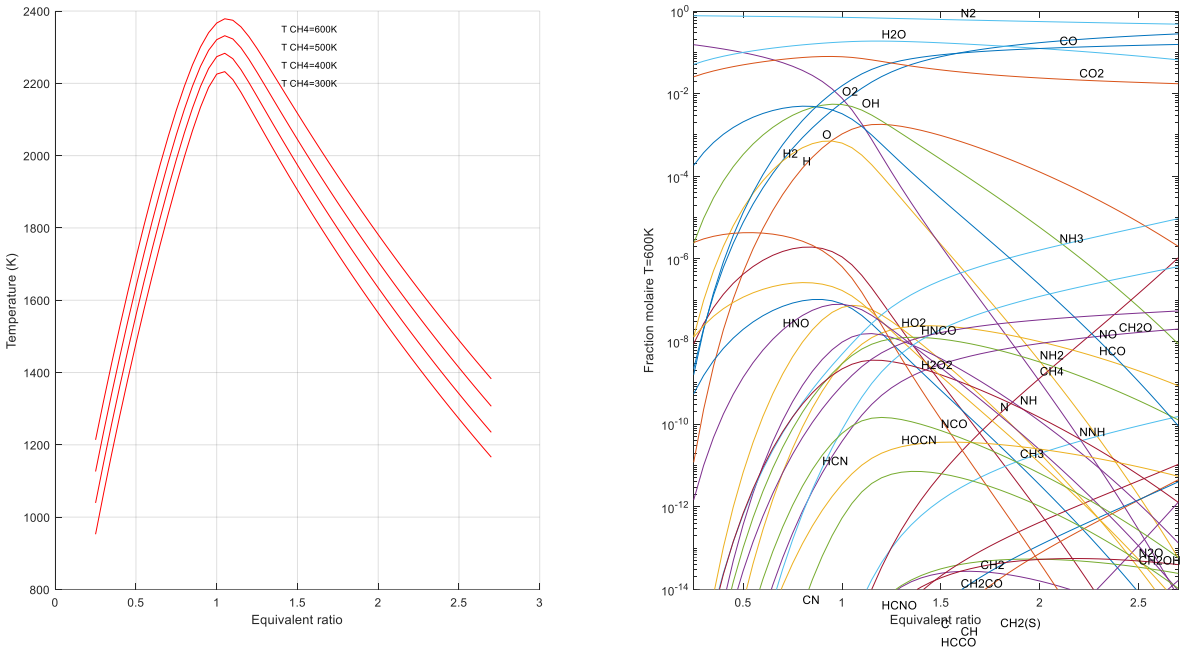


Fig .2 Temperature dynamic / equivalence ratio.

The oscillations of $\dot{m}_o$ and $\dot{m}_f$ are produced by an unstable combustion dynamic. The periodic combustion process causes an acoustic fluctuation to be propagated into the inlet (see Fig.1) and produces oscillations in velocity and, thus, mass flow rate of the oxidizer $\dot{m}'_o$ at the fuel injection. In addition, if the inlet fuel is un-choked, pressure oscillations in the inlet duct produce fuel flow-rate oscillations $\dot{m}'_f$. Inside the combustion zone, the variation of control variable ϕ causes a heat-release rate of the reactants (See Fig.3).

Since the thermo-acoustic instabilities depend on heat discharge, it is assumed that the magnitude will rise in proportion to the equivalency ratio. The flame propagates, increasing the pressure perturbation cross the axis x when the boundary condition will reduce their amplitudes. The Cantera algorithm and data from the representative chemical species were

used to create the chemical composition table [20].The part inside the single quotes specifies that the species, kinetics, and thermodynamics are calculated according to the GRI 3.0 mechanism for methane.

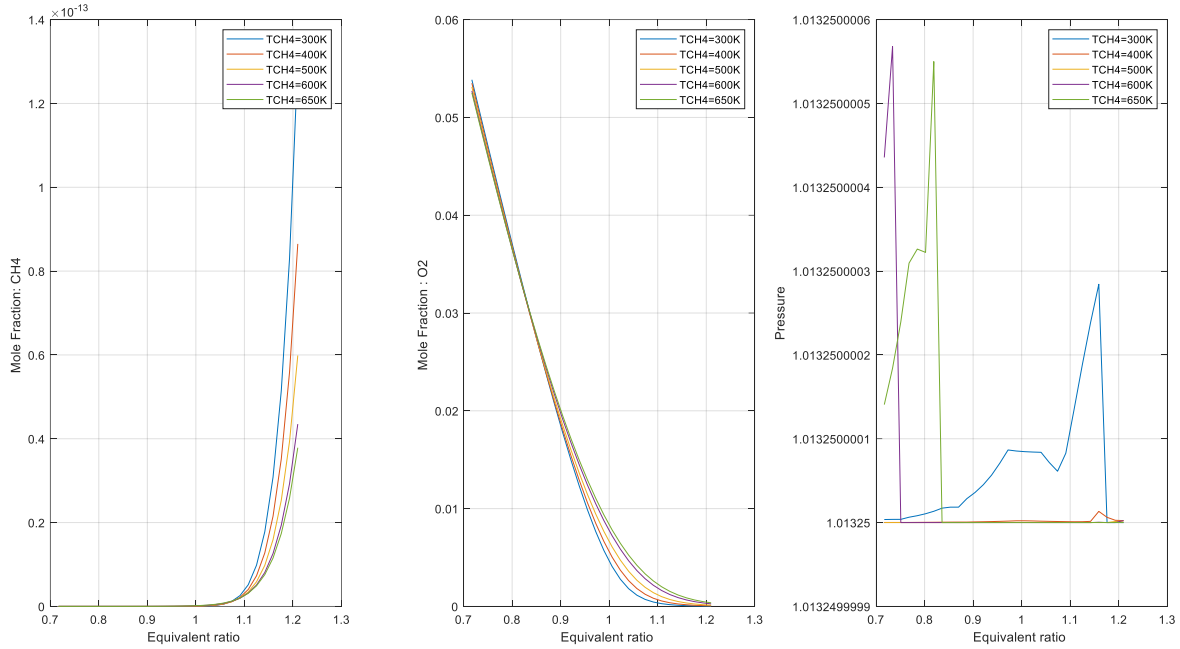


Fig .3 Mole fractions and pressure dynamics / equivalence ratio [0.7,1.2]

2.2 Thermo-acoustic waves

The flow average range is especially important inside the combustor control zone, and it is assumed that the control zone is little in comparison to the length of acoustic waves. It is supposed that the flow disturbances are modelled as one-dimensional entropy waves and one-dimensional acoustic waves propagating in two directions and convicting the downstream of controlled volume. The flow disturbances are linearized around an average value, and all average values are noted by overbar as $\bar{c}$ representing the speed of sound in the case of stationary fluid. In region I, upstream of the combustion zone, the equations for the pressure, density, and velocity take the form [21]:

$$\boldsymbol{Pressure}: \quad p(x,t) = \bar{p}_1 + A\left(t - \frac{x}{\bar{c}_1 + \bar{u}_1}\right) + B\left(t + \frac{x}{\bar{c}_1 - \bar{u}_1}\right) \tag{6}$$

$$\boldsymbol{Density}: \quad \rho(x,t) = \bar{\rho}_1 + \frac{1}{\bar{c}_1{}^2}\left[A\left(t - \frac{x}{\bar{c}_1 + \bar{u}_1}\right) + B\left(t + \frac{x}{\bar{c}_1 - \bar{u}_1}\right)\right] \tag{7}$$

$$\boldsymbol{Velocity}: \quad u(x,t) = \bar{u}_1 + \frac{1}{\bar{\rho}_1 \bar{c}_1}\left[A\left(t - \frac{x}{\bar{c}_1 + \bar{u}_1}\right) + B\left(t + \frac{x}{\bar{c}_1 - \bar{u}_1}\right)\right] \tag{8}$$

The downstream of the combustion region II and III, possess the subsequent structure, where the specific heat capacity at constant pressure is represented by c_p and the amplitude of the entropy wave by σ.

$$\boldsymbol{Pressure}: \quad p(x,t) = \bar{p}_2 + D\left(t - \frac{x}{\bar{c}_2 + \bar{u}_2}\right) + E\left(t + \frac{x}{\bar{c}_2 - \bar{u}_2}\right) \tag{9}$$

$$\textbf{Density}: \quad \rho(x,t) = \bar{\rho}_2 + \frac{1}{\bar{c}_2{}^2}\left[D\left(t - \frac{x}{\bar{c}_2 + \bar{u}_2}\right) + E\left(t + \frac{x}{\bar{c}_2 - \bar{u}_2}\right)\right] - \frac{\bar{\rho}_2}{c_p}\sigma\left(t - \frac{x}{\bar{u}_2}\right) \tag{10}$$

$$\textbf{Velocity}: \quad u(x,t) = \bar{u}_2 + \frac{1}{\bar{\rho}_2\bar{c}_2}\left[D\left(t - \frac{x}{\bar{c}_2 + \bar{u}_2}\right) + E\left(t + \frac{x}{\bar{c}_2 - \bar{u}_2}\right)\right] \tag{11}$$

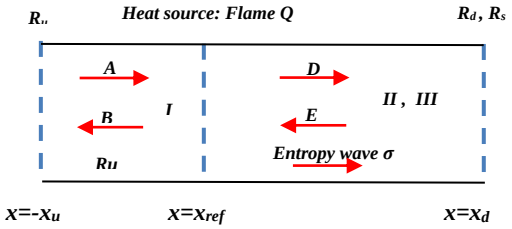


Fig. 4 Schematic of a ducted flame combustor

The fluid upstream and downstream of the flame is considered a perfect gas, and cross the duct, the specific heat is considered constant. For an open duct at both ends, we referred to a Rijke tube. The mathematical representation and values of wave amplitudes (*A*,*B*,*D*,*E*) within each region can then be found in [21].

3 Thermo-acoustic model stability

This subsection's goal was to demonstrate how to attenuate combustor instability under circumstances that were comparable to those found in a real aircraft engine (e.g., the operating points, the frequency of instability, and the magnitude of instability are identical). As a result, test cases 1 and 2 are considered to demonstrate the various effects of time-varying flame position can have on combustor stability. Table 2 depicts the combustor geometries, Mach number, and coefficients of boundary reflection. The envelopes of the associated pressure oscillations are depicted in Figs. 5, 6, and 7 where the normalised acoustic pressure, p_{ref} , at location x_{ref} given.

Table. 2 Combustor parameters used in test cases

.Case	$x_u[m]$	$x_d[m]$	$x_{ref}[m]$	R_-	R_+	M_-
1	-0.3	0.841	0.33	-1	-1	0.08
2	-1.5	0.6855	0.22	0.85	-0.98	0.08
3	-1.0	1.2	0.33	0.85	-0.98	0.08

For three unstable cases, the limit cycle is simulated, where a suppressed upstream boundary is used for the upstream reflection coefficient. To ensure uniformity with the open end condition, the downstream limit condition could be changed, but it was always considered a negative number.

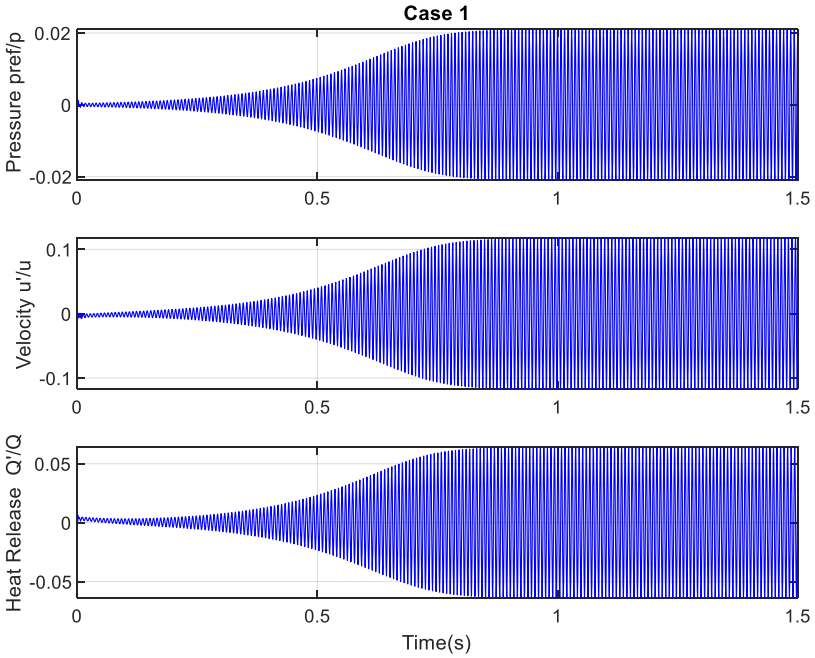


Fig. 5 Behavior of limit cycle without control: case 1

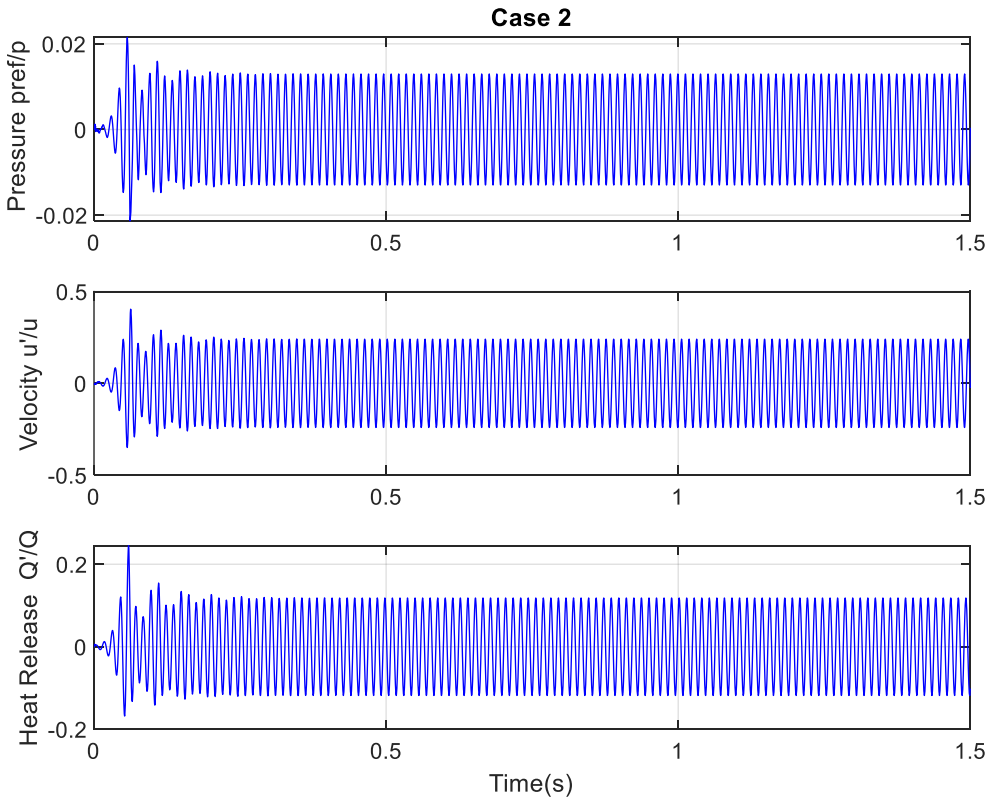


Fig. 6 Behavior of limit cycle without control: case 2

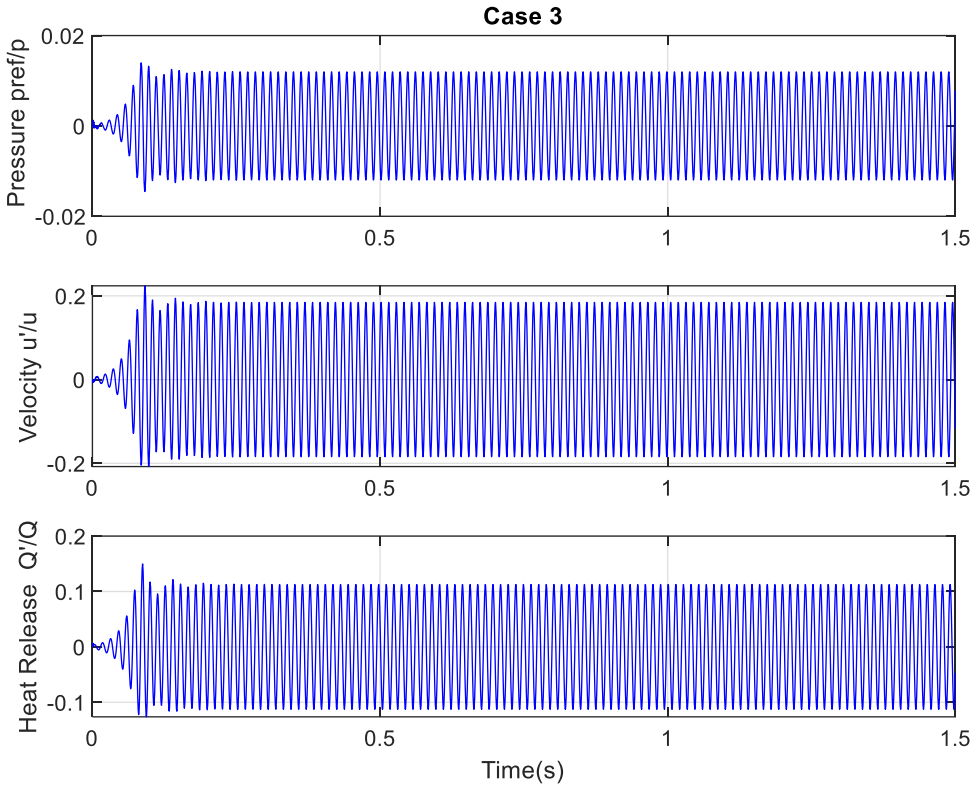


Fig. 7 Behavior of limit cycle without control: case 3

4 Feedback active control

Feedback control is used to deal with a wide range of operating conditions, especially when a nonlinear control methodology is considered, and it needs little space compared to bulky acoustic dampers that absorb low-frequency combustion oscillations. The feedback control is chosen for its accurate measurement of a reference signal and actuates some system energies. Accurate sensing and actuation are necessary closed-loop control of combustion oscillations makes the control system more challenging [1]. Furthermore, sensing and actuation issues complicate the design of an effective and robust controller, the prevalent variation in operating ranges, and the different sources and dynamics of combustion instabilities in different features of industrial combustors [1].

4.1 Sensors and actuators

Pressure sensors are the best choice for a practical active control of thermos-acoustics because of their large bandwidth as well as acceptable robustness. Since the acoustic perturbations are spread across all the combustor volume, the sensors can be placed in several positions, especially far from the high temperature zone. In practice, a properly designed actuator is much more unexpected to require control specifications. The active actuator, as a solenoid valve, modifies the air/fuel or equivalence ratio. The linear dynamic response of the solenoid valve gives the possibility for this actuator to be used in extended scale or even complete scale implementation, but it has two main drawbacks: 1) its restricted bandwidth and 2) control weighting. Consequently, magneto-resistive has been shown to be promising in practical application (full-scale) for its increased bandwidth, as long as the control frequency weighting is kept high. The actuator transfer function of $W_{ac}(s)=\frac{1}{3.166e-8S^2+0.0003581S+1}$ was used for all three cases, involves varying the fuel flow rate in response to pressure readings.

4.2 The controller architecture

It's critical to understand the bandwidth frequency and magnitude of a thermo-acoustics model. for designing a combustor in any industrial field [21]. Obtaining linear model or a using a nonlinear controller is much more difficult if the system had limit cycle behavior. The practical operating conditions of the combustor, as is the case combustion engine during the transition from start to stationary regime, can reduce the performances of the controller and attenuate the reliability, or even worse, it could further conduct the combustor to instable behavior [6]. The combustion instability remains one of the most difficult challenges facing lean combustion [21]. As a result, we proposed an adaptive fuzzy-neural controller capable of dealing with instabilities (Limite cycles), achieving fast response, good transient performance, and robustness in the face of variations in the operating conditions of the combustor and modelled disturbances [1,21]. The dynamical processes in large- and full-scale combustion systems are too complex for physics-based models to be useful. As a result, system identification techniques are required for model-based control to mitigate combustion instability. [1,21].

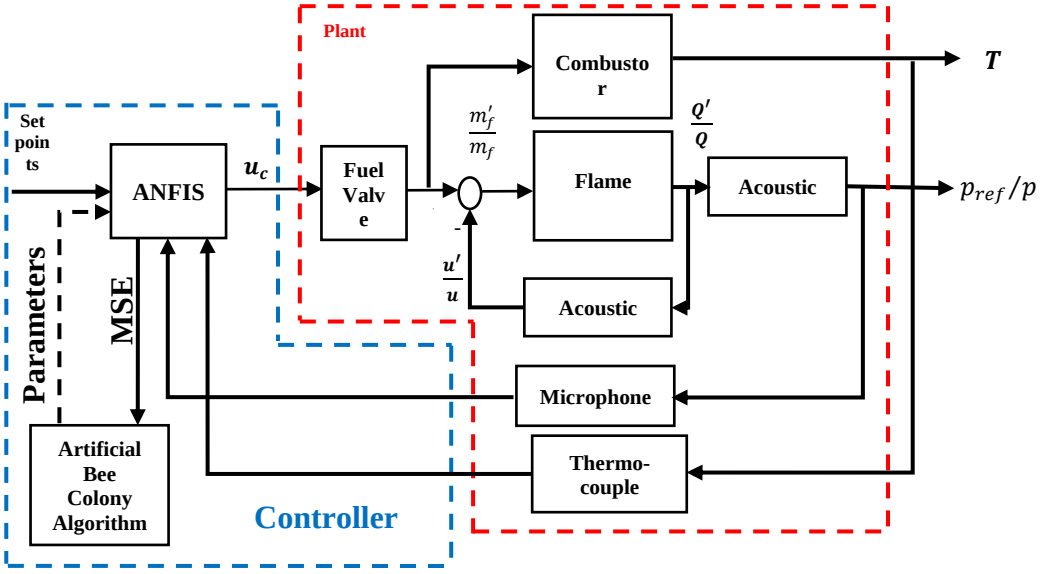


Fig. 8 Block diagram representation of the proposed control architecture

4.3 ABC neuro-fuzzy controller

Neuro-fuzzy inference machine is an adaptable approach made up of two parts: an artificial neural network and a fuzzy inference system. ANFIS gathers the benefits of artificial neural networks as well as traditional fuzzy words. ANFIS structure training is a subset of optimization problems. Metaheuristics and evolutionary algorithms can be used to train (adjust the parameters of) an ANFIS structure. The evolutionary-trained ANFIS is used to solve a mathematical model, including nonlinear modeling and function approximation. Fuzzy rules were generated from numerical input by the neural network system and, in the learning process phase, the membership functions were automatically updated. A Sugeno fuzzy model with two inputs e_T and e_P, and one output f is considered. For the proposed case, the fuzzy rules are considered as following:

$$\begin{aligned} &Rule\ I: if\ e_T = A_1\ and\ e_P = B_1, then\ f_1 = p_1 e_T + q_1 e_P + r_1 \\ &Rule\ II: if\ e_T = A_2\ and\ e_P = B_2, then\ f_2 = p_2 e_T + q_2 e_P + r_2 \end{aligned} \tag{12}$$

where, f is the controller response, p, q, and r are linear parameters, and A and B are nonlinear parameters. Fig.9 depicts the five layers that were used to design the ANFIS structure, with

each layer being used as follows: ***Layer 1:*** input nodes, ***Layer 2*****:** rule nodes: ***Layer 3:***average nodes, ***Layer 4:*** consequent nodes, ***Layer 5:*** output nodes. The control signal of ANFIS can be found as a linear combination of the consequent parameter, and the control mathematical expression can be written as [22]:

$$f_{out} = \overline{w}_1 f_1 + \overline{w}_2 f_2 = \frac{w_1}{w_1 + w_2} f_1 + \frac{w_2}{w_1 + w_2} f_2 = (\overline{w}_1 x) p_1 + (\overline{w}_1 y) q_1 + (\overline{w}_1) r_1 + (\overline{w}_2 x) p_2 + (\overline{w}_2 y) q_2 + (\overline{w}_2) r_2 \quad (13)$$

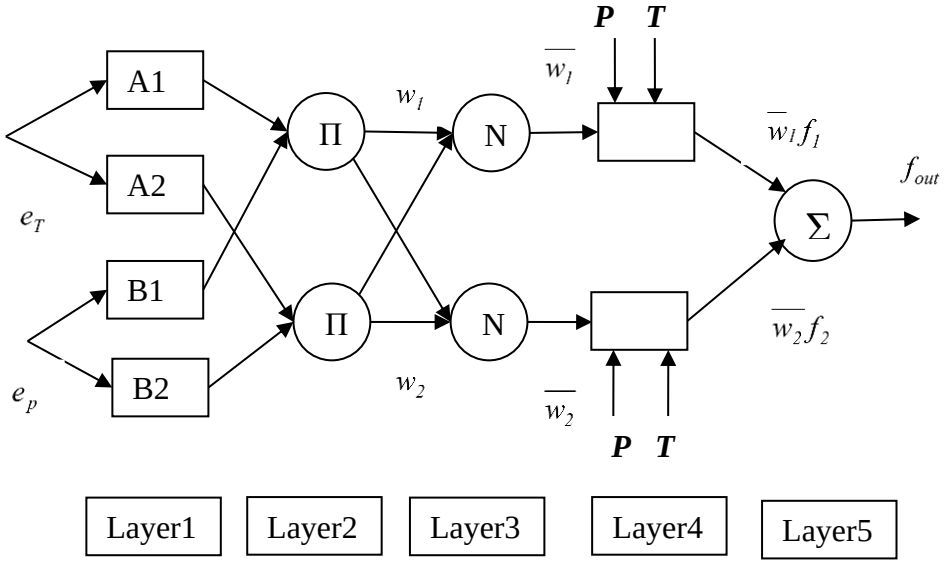


Fig.9 Neuro-fuzzy controller architecture

ABC is used to adjust the settings of the ANFIS controller's membership functions to improve the control process [22]. The bee colony is composed of employed bees, onlooker bees, and scout bees, Assuming that i^{th} solution of food source population represented by $X_i = \{x_{i,1}, x_{i,2}, \cdots x_{i,n}\}$. Where V_i is a new neighbourhood solution for the employed bee as in the equation below:

$$v_{i,k} = x_{i,k} + \Phi_{i,k} \times (x_{i,k} - x_{j,k}) \quad (14)$$

where X_j is a random selection of the possible sources ($i \neq j$), k is selected from the set $\{1,2,\cdots n\}$, and $\Phi_{i,k}$ is a random selection between -1 and 1. X_i can be replaced by V_i, when the cost of V_i is better than the parent X_i. After all employed bees have achieved the search; they report the location of the found food sources with onlooker bees via dances. An onlooker bee assesses the nectar data collected from all employed bees and selects a food source with a probability proportional to its nectar quantity. The chosen selection process is the roulette wheel illustrated by the following equation [23]:

$$P_i = \frac{fit_i}{\sum_j fit_j} \quad (15)$$

where fit_i is the fitness value of the i^{th} solution in the set. The best probability of the i^{th} food source is selected. If a position cannot be improved after a predetermined number of

cycles (called the limit), the food source is abandoned. If the abandoned source is X_i, and then the scout bee discovers a new food source to be replaced with i^{th} as equation below:

$$x_{i,k} = lb_k + \Phi_{i,k} \times (ub_k - lb_k)$$

where $\Phi_{i,k} = rand(0,1)$ is a normal distribution, lb_k and ub_k are lower and upper boundaries of the k^{th} dimension, respectively [23]. The ABC algorithm optimizes the following integral square error cost (ISE) function to compute the appropriate clustering of membership function of the ANFIS controller:

$$J = \int_0^\infty (e_T(t))^2 + (e_p(t))^2 + (\dot{m}_f(t))^2 + (\dot{m}'_f(t))^2 \quad (16)$$

where e_T, e_p are the temperature and pressure error, and $\dot{m}_f$, $\dot{m}'_f$ are fuel mass flow and flow mass flow fluctuation respectively.

5 Simulation and results

The performance of ANFIS controller is demonstrated on a chemical/thermo-acoustic lumped model simulation. It is desirable to get an estimate of the P_{ref} value of the acoustic signature in steady state for an unknown operating condition while running/designing a combustor. This is due to the fact that P_{ref} is directly related to the level of limit cycle instability; a greater P_{ref} suggests a more unstable system [24].

The mean squared error is close to zero in Fig.10, and Fig.11 demonstrates the velocity of ABC algorithm convergence and exploitation while managing the compromise between exploration and exploitation within a multidirectional research space. The suggested ABC optimization can optimize the ANFIS controller's setting, according to these two figures, which show that the controller was sufficiently taught with few errors.

To highlight the adaptability of the proposed control design, we display the optimization results (in Fig.12) to show how membership functions are tuned using the gaussmf membership function for the inputs and a linear membership function for the output, each having 10 rules. The iteration length used is 100 iterations for each sample. Small white noise background disturbances are found in Fig.13. Starting from *t=0*, the perturbation decreased rapidly compared to the perturbation when the control was off, as illustrated in Fig.5, Fig.6 and Fig.7, with a limit cycle that disappeared approximately beyond *t*=0.05s, as illustrated in Fig.13.

The ABC algorithm provides an improvement, by comparing ANFIS performance with the same ANFIS optimized by ABC, a significant increase of time stabilisation (Fig.13). A clear improvement of the response time and fuel consumption is thus visible. An ABC exploration of this search space is conducted to identify more relevant and accurate subsets of parameters through a new distribution of the membership function, which adapts well to each linguistic variable, which leads to minimizing the error between the desired trajectory and the calculated one.

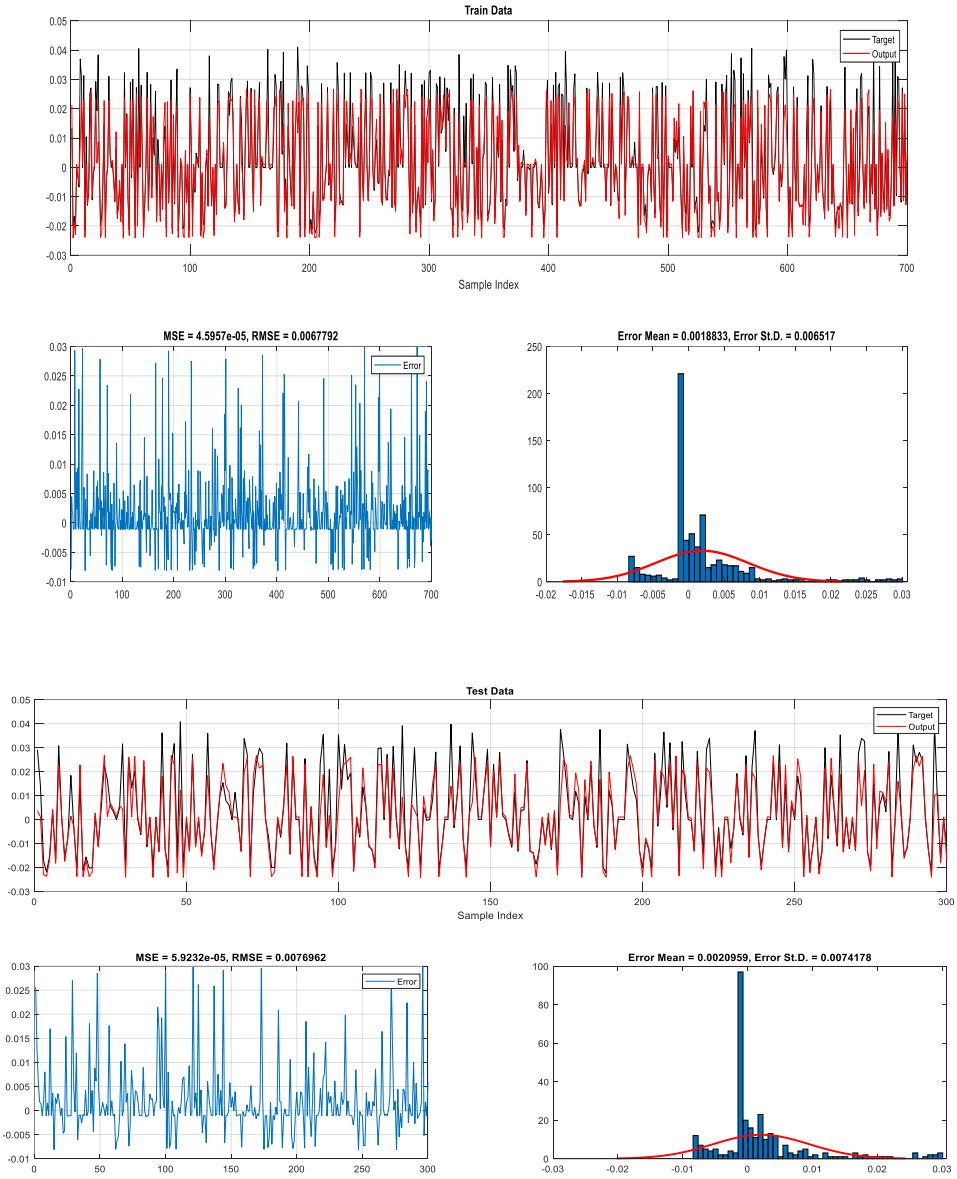


Fig.10 MSE of train and test

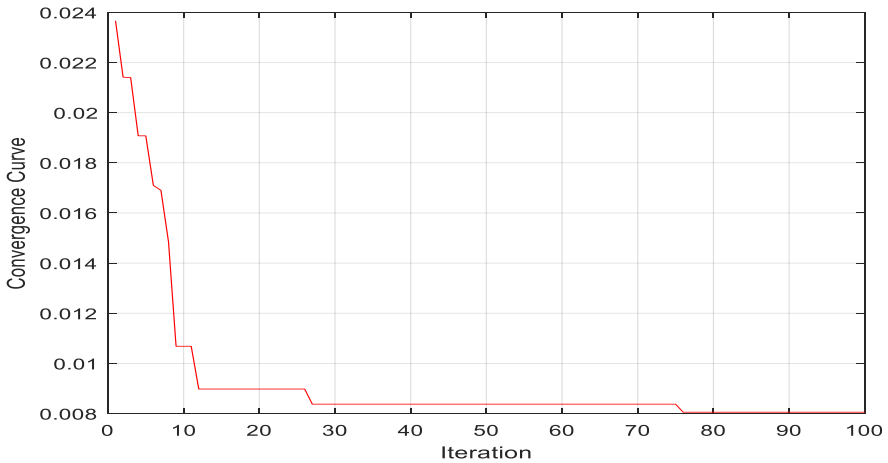


Fig.11 Convergence Curve of ABC Algorithm

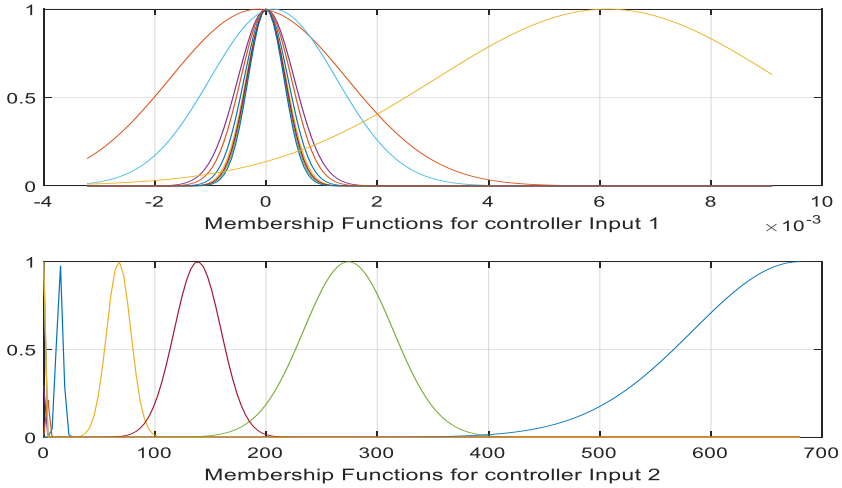


Fig.12 The optimized membership functions

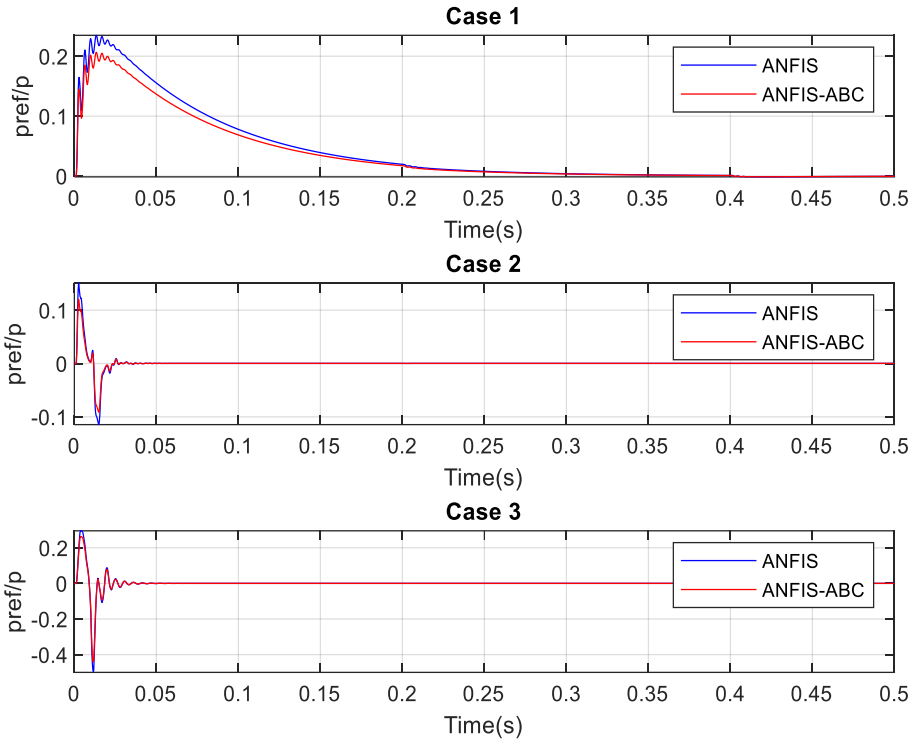


Fig.13 Envelope of the normalized pressure for the 3 cases

Fig.14 depicts a dynamic simulation of the combustion reaction; first, the temperature rises fast before reaching a stationary level [25], and secondly, for a continuous operating case with vanished thermos-acoustic instabilities, the combustion temperature stays constant close to 1280K. In Fig.15 and Fig.16, the mass fractions of the fuel and oxidizer fall fast and eventually stabilize near zero. This result implies that about all of the fuel and oxidizer are converted to products, which is compatible with the fuel/oxidizer ratio, which was set to be close to the stoichiometric value. This lends support to the hypothesis that the exhaust fluid is largely made up of combustion products [25]. The fuel fluctuation grows in proportion to the amplification of the pressure perturbation. As a result, heat generation has increased. Fig.18 also depicts the temperature's time response [25]with various equivalence ratios.

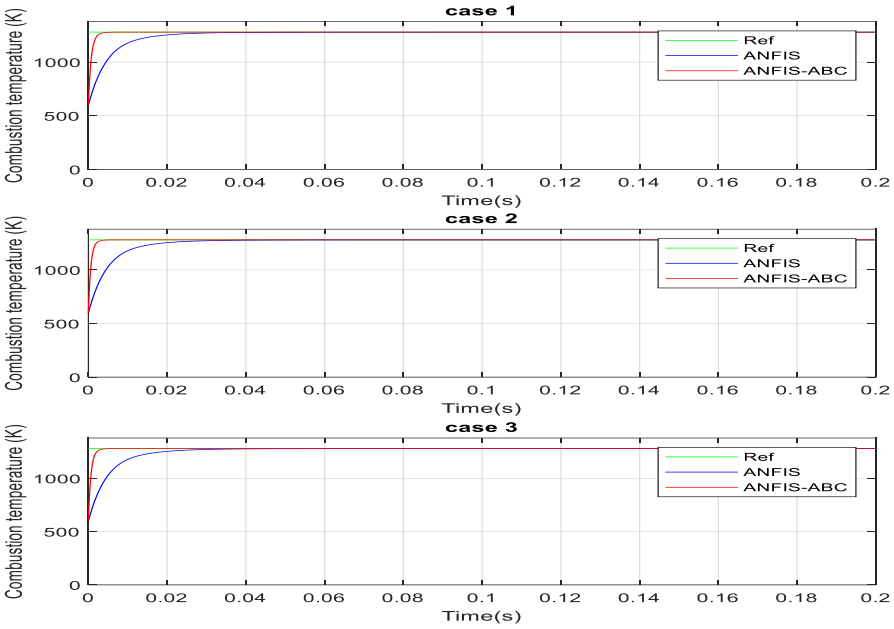


Fig.14 Combustion dynamic: Combustion temperature

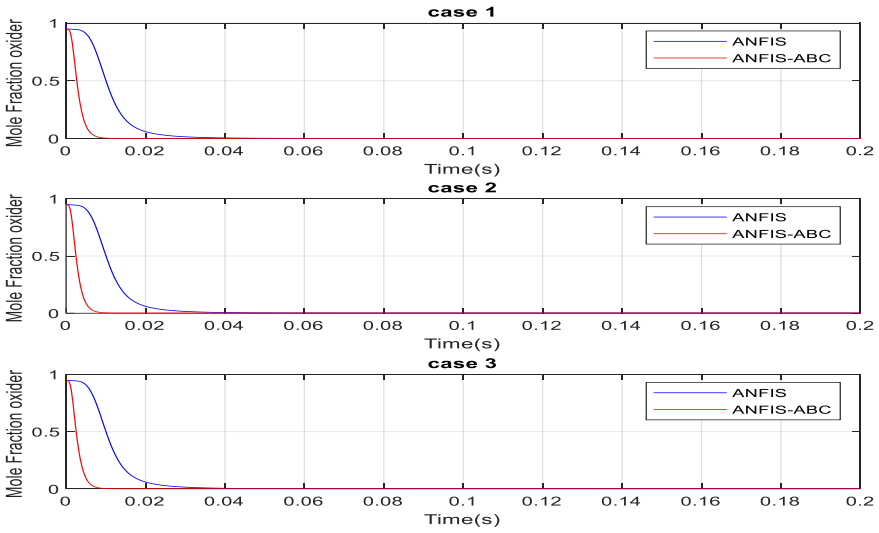


Fig.15 Combustion dynamic: Mole fraction of oxidizer

To keep the combustor within a stable envelope, the ABC-ANFIS controller produces an equivalency that varies between 0.7 and 1. The combustion temperature rises with increasing equivalence ratio, as illustrated (supposition of Fig.14 and Fig.18), because the amount of energy that can be converted reduces with decreasing equivalence ratio.

The temperature of the combustor model is explored as an adiabatic flame temperature if the combustor is considered an adiabatic reactor. Furthermore, because the combustor is supposed to be a well-stirred reactor, the equivalence ratio change is regarded as the most effective actuation parameter utilized to stabilize the instantaneous temperature inside the combustor.

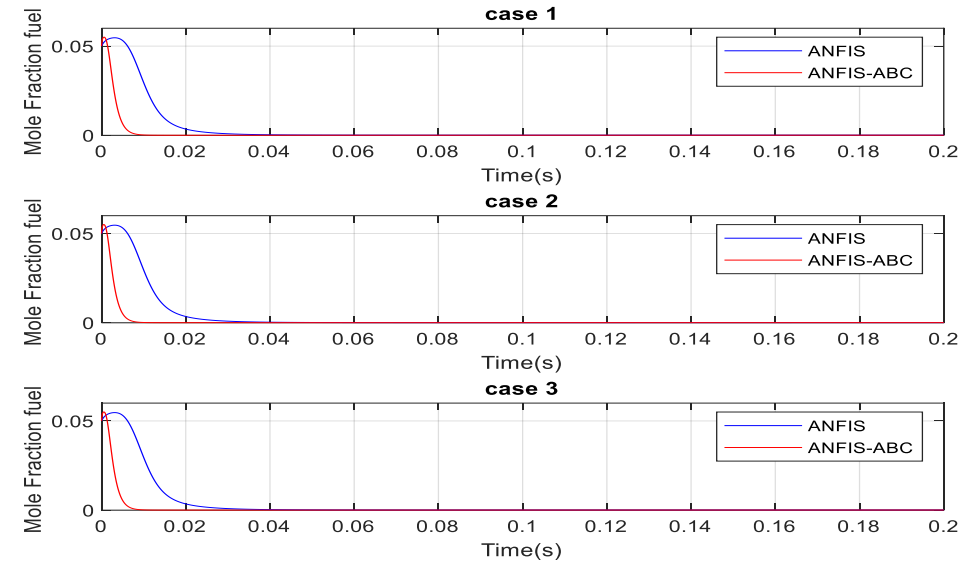


Fig.16 Combustion dynamic: Mole fraction of fuel

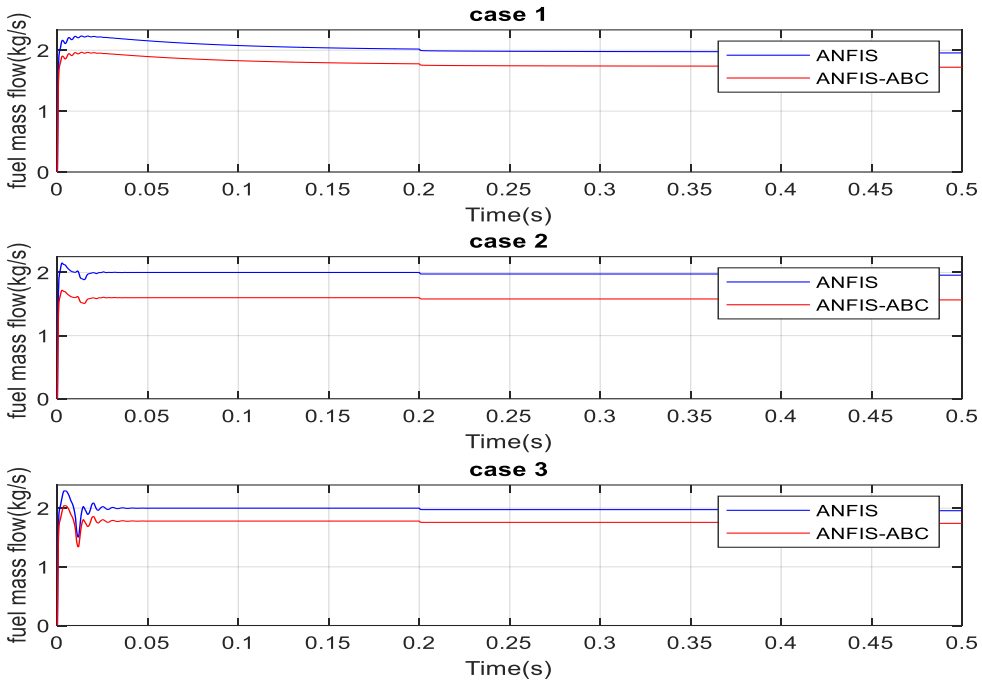


Fig.17 Combustion dynamic: fuel mass Flow (Control effort)

CONCLUSION

This research focuses on the neuro-fuzzy approach's ability to detect and stabilize thermo-acoustic instabilities. An ANFIS methodology is proposed; through which ABC optimization achieves stability in a lean premixed combustion condition. A well-stirred reactor configuration anticipates and eliminates the level of instability for a variety of operating conditions. The results clarify that an ABC-ANFIS controller can be used to control the temperature of systems ranging from simple to sophisticated combustion systems. It also emphasizes the ease of use of such a control methodology in suppressing flame perturbation instability in a wide variety of operating situations, which has the potential to expedite and improve engine design and performance. The model was trained with a relatively limited volume of data on one example and applied to operate the system in three cases, making the

problem more difficult and introducing complexity such as employing industrial combustion systems for which full scale training data would not be accessible.

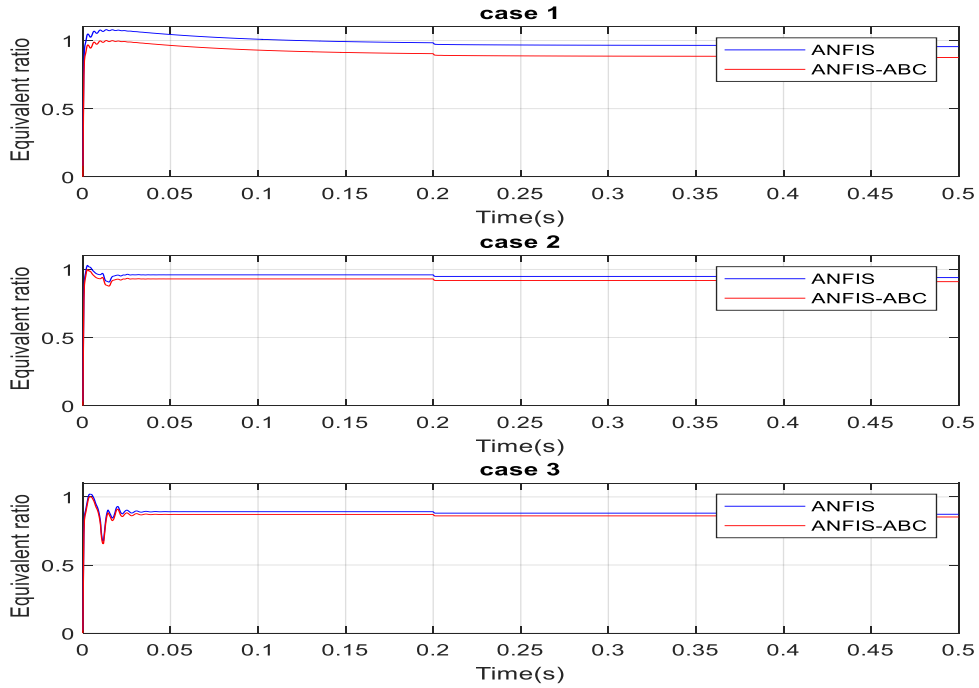


Fig.18 Combustion dynamic: Equivalence ratio

REFERENCES

[1] Zhao, D., Lu, Z., Zhao, H., Li, X. Y., Wang, B., Liu, P. "A review of active control approaches in stabilizing combustion systems in aerospace industry", Progress in Aerospace Sciences, 97, pp.35 – 60, **2018**. DOI: 10.1016/j.paerosci.2018.01.002

[2] Andrej, C.,Marián, P. Matej, M. "Use of Methane-Free Synthesis Gases as Fuel in an Spark Ignition Combustion Engine", Strojnícky časopis – Journal of Mechanical Engineering 70(2), pp. 37 – 48, **2020**. DOI: 10.2478/scjme-2020-0018

[3] Fougnie, A., Schmitt, T., Ducruix, S. "Analysis and low order modeling of the acoustic damping for high-frequency combustion instabilities prediction in liquid rocket engines", in space propulsion, **2022**. Available at: https://hal.archives-ouvertes.fr/hal-03676560 /document. [Accessed: date (20/08/2022)]

[4] Olgac, N., Zalluhoglu, U., Kammer, A. S. "A new perspective in designing delayed feedback control for thermo-acoustic instabilities (TAI) ", Combustion Science and Technology 187(5), pp.697 – 720, **2015**. DOI: 10.1080/00102202.2014.960924

[5] Zalluhoglu, U., Kammer, A. S., Olgac, N. "Delayed feedback control laws for Rijke tube thermoacoustic instability, synthesis, and experimental validation", IEEE Transactions on Control Systems Technology 24(5), pp. 1861 – 1868, **2016**. DOI: 10.1109/tcst.2015.2512938

[6] Illingworth, S. J., Morgans, A. S. "Adaptive feedback control of combustion instability in annular combustors", Combustion science and technology 182(2), pp. 143 – 164, **2010**. DOI: 10.1080/00102200903258773

[7] Paredes, J. A., Ramesh, R., Obidov, S., Gamba, M., Bernstein, D. "Experimental Investigation of Adaptive Feedback Control on a Dual-Swirl-Stabilized Gas Turbine Model Combustor", In: AIAA SCITECH 2022 Forum, San Diego, CA & Virtual, pp. 2022 – 2058, **2022**. DOI: 10.2514/6.2022-2058.

[8] Machesa, M. G. K., Tartibu, L. K., Tekweme, F. K., Okwu, M. O. "Prediction of oscillatory heat transfer coefficient in heat exchangers of thermo-acoustic systems", In: ASME International Mechanical Engineering Congress and Exposition, Salt Lake City, UT, USA, pp.59452, p. V008T09A043, **2019**.

[9] Ngcukayitobi, M., Sibutha, S., Tartibu, L. K., Bannwart, F. C. "Performance analysis of a two-stage travelling-wave thermo-acoustic engine using Artificial Neural Network", In : MATEC Web of Conferences 347, EDP Sciences, **2021**. DOI: 10.1051 /matecconf/202134700023

[10] Milesich, T., Danko, J., Bucha, J. "Neural Networks-A Way to Increase the Fuel Efficiency of Vehicles", Strojnícky časopis – Journal of Mechanical Engineering 68(1), pp. 81 – 88, **2018**. DOI: 10.2478/scjme-2018-0008

[11] Niederberger, A. S., Fritsche, D., Boulouchos, K., Guzzella, L. "Thermoacoustic Instability Suppression by Gain-Delay and H∞ Controllers Designed for Secondary Fuel Injection", IEEE transactions on control systems technology 17(5), pp. 1028 – 1042, **2009**. DOI: 10.1109/TCST.2008.2004809

[12] Feng, S., Li, J. "H∞ loop-shaping control of azimuthal combustion instabilities in annular combustors. Journal of Low Frequency Noise", Vibration and Active Control, 40(1), pp.395-412, **2021**. DOI: 10.1177/1461348419873455

[13] Yuan, X. C., Glover, K. "Model-based control of thermoacoustic instabilities in partially premixed lean combustion–a design case study", International Journal of Control 86(11), pp. 2052 – 2066, **2013**. DOI: 10.1080/00207179.2013.830337

[14] Norouzi, A., Heidarifar, H., Shahbakhti, M., Koch, C., R.; Borhan, H. "Model Predictive Control of Internal Combustion Engines: A Review and Future Directions", Energies 14, pp. 6251, **2022**. DOI: 10.3390/en14196251

[15] Yazar, I., Caliskan, F., & Vepa, R. "Model Predictive Control and Controller Parameter Optimisation of Combustion Instabilities", International Journal of Turbo & Jet-Engines 36(2), pp. 185 – 194, **2019**. DOI: 10.1515/tjj-2017-0062

[16] Alsuwian, T., Tayyeb, M., Amin, A. A., Qadir, M. B., Almasabi, S., Jalalah, M. "Design of a Hybrid Fault-Tolerant Control System for Air–Fuel Ratio Control of Internal Combustion Engines Using Genetic Algorithm and Higher-Order Sliding Mode Control", Energies 15(15), pp. 5666, **2022**. DOI: 10.3390/en15155666

[17] Debbah, A., Kherfane, H., Klaiaia, R. "Gas Turbine Aerodynamics Improvement Via a Design of Intelligent Fractional Control", Strojnícky časopis – Journal of Mechanical Engineering 71(2), pp. 85 – 100, **2021**. DOI: 10.2478/scjme-2021-0020

[18] Debbah, A., Kherfane, H. "GA/PSO robust sliding mode control of aerodynamics in gas turbine", Acta Universitatis Sapientiae, Electrical and Mechanical Engineering 10(1), pp. 42 – 66, **2018**. DOI: 10.2478/auseme-2018-0003

[19] Procházka, R., Dittrich, A., Beroun, S., Zvolský, T., Voženílek, R. "The Working Cycle of the Motoring Internal Combustion Engine by a New Method with Cylinder Pressures as in Real Engine Operation", Strojnícky časopis – Journal of Mechanical Engineering 72(3), pp. 41 – 52, **2022**. DOI: 10.2478/scjme-2022-0039

[20] Han, J., Jeong, J. Cho, K., Yu, S. "A Real-Time Combustion Instability Simulation with Comprehensive Thermo-Acoustic Dynamic Model", Energies 11(4), pp. 883 – 904, **2018**. DOI: 10.3390/en11040883

[21] Yang, D., Laera, D., Morgans, A. S. "A systematic study of nonlinear coupling of thermoacoustic modes in annular combustors", Journal of Sound and Vibration 456, pp. 137 – 161, **2019**. DOI: 10.1016/j.jsv.2019.04.025

[22] Euldji, R., al. "Optimal ANFIS-FOPID with back-stepping Controller design for wheeled Mobile Robot control", Journal of Control Engineering and Applied Informatics 24(2), pp. 57 – 68, **2022**. DOI: 10.18280/jesa.550110

[23] Kumar, A., Dharmender, K., Jarial, S. K."A review on artificial bee colony algorithms and their applications to data clustering", Cybernetics and Information Technologies, 17(3), pp. 3 – 28, **2017**. DOI: 10.1515/cait-2017-0027

[24] Han, X., Li, J., Morgans, A. S. "Prediction of combustion instability limit cycle oscillations by combining flame describing function simulations with a thermoacoustic network model", Combustion and Flame 162(10), pp. 3632 – 3647, **2015**. DOI: 10.1016/j.combustflame.2015.06.020

[25] Chribik, A., Minárik, M., Polóni, M. "Effect of Selected Components on Combustion of Methane" Strojnícky časopis – Journal of Mechanical Engineering 71(2), pp. 61 – 68, **2021**. DOI: 10.2478/scjme-2021-0018

Nomenclature

Variable	Designation
A,B,D,E	wave amplitudes
c_p	Specific heat capacity [J.kg $^{-}$1.K^{-1}]
c	Sound velocity [ms^{-1}]
$\dot{m}$	Mass flow rate [kg.s^{-1}]
MW_{fuel}	Molecular weight of fuel (Methane) [kg.kmol^{-1}]
p	Pressure [kPa]
Q	Heat release rate [kJ.s^{-1}]
R_u, R_d	Acoustic reflection coefficients at the upstream and downstream
R_s	Acoustic reflection coefficient from the entropy wave
T	Temperature [K]
t	Time [s]
τ	Time delay [s]
u	Average of the mean flow [ms $^{-1}$]
V_{cc}	Volume of combustion chamber[m^3]
w	Acoustic mode frequency [Hz]
Y	Mass fraction
ρ	Density [kg.m^{-1}]
ϕ	Equivalence ration
$\dot{\omega}_{fuel}$	Arrhenius rate term for consumption of species due to combustion
Subscripts and Superscripts	
fuel or *f*	Fuel
i	Chemical species
in	Inlet flow
mix	Mixture
oxid	Oxidizer
prod	Products
ref	Reference